An Analytical Model for Skylight Polarisation

A. Wilkie[1] and C. Ulbricht[1] and Robert F. Tobler[2] and G. Zotti[1] and W. Purgathofer[1]

[1] Institut für Computergraphik und Algorithmen, TU Wien, Austria
[2] VRVis Research Center, Austria

Abstract

Under certain circumstances the polarisation state of the illumination can have a significant influence on the appearance of scenes; outdoor scenes with specular surfaces – such as water bodies or windows – under clear, blue skies are good examples of such environments. In cases like that it can be essential to use a polarising renderer if a true prediction of nature is intended, but so far no polarising skylight models have been presented.
This paper presents a plausible analytical model for the polarisation of the light emitted from a clear sky. Our approach is based on a suitable combination of several components with well-known characteristics, and yields acceptable results in considerably less time than an exhaustive simulation of the underlying atmospheric scattering phenomena would require.

Categories and Subject Descriptors (according to ACM CCS): I.3.7 [Computer Graphics]: Three-Dimensional Graphics and Realism

1. Introduction

In recent years several key improvements to the realism of synthetic outdoor scenes have been made. They covered diverse areas such as rendering algorithms, tone mapping [PFFG98] and actual skylight models [PSS99], and in some areas such as spectral rendering the community is only now starting to routinely use methods which have been known for a long time [HG83].

Although a high level of visual realism has already been reached through these improvements, current systems are still not capable of truly predictive rendering of outdoor scenes. Our aim is to address one of the remaining shortcomings in this area.

The use of polarization information during image synthesis calculations has lain dormant for more than a decade after its principles were established [WK90]. Apart from the fact that it is very computationally intensive, it has received little attention in the rendering community because – while of course being essential for specially contrived setups that for instance contain polarizing filters – its addition normally does not contribute very prominent effects to the appearance of an average indoor scene.

However, one of the main areas where polarisation in fact can make a substantial difference to the overall radiance distribution are outdoor scenes; this is due to the – under certain circumstances quite strong – natural polarisation of skylight. The resulting visual artefacts are so diverse that entire books have been devoted to their documentation [Kön85]. And the effects of these atmospheric phenomena are not limited to direct viewing of the sky.

Strongly specular surfaces such as water bodies, windows, car roofs or wet road surfaces best reflect horizontally polarised light. Since skylight can be strongly vertically polarised for certain viewing geometries, it is only poorly reflected in these cases, and the mirror image of the sky is noticeably different from the results obtained with a plain light model. As a consequence, the entire energy distribution in a scene can be wrong, which can be all the more significant when using a modern global illumination rendering algorithm which takes multiple interreflections into account.

Since outdoor scenes are currently still problematical for photorealistic renderers for a number of other, more obvious reasons (e.g. scene complexity and related global illumination issues), this whole problem domain has not been given a lot of attention yet. Also, although comparatively

sophisticated analytical skylight models which are even partially based on spectral radiance measurements have been presented recently [PSS99], no mathematical description of the polarisation patterns found in a clear sky – as shown e.g. in figures 2 and 3 – has been presented so far. In this paper we attempt to fill this gap.

2. Background

2.1. Skylight models

A number of analytical models have been developed to describe sky radiance and its spectral radiance in the context of photorealistic image synthesis; we just give a brief overview over those models which are of direct interest to our approach since we based our derivations and implementation on some of them.

It should be noted that there exists a significant body of additional work on this topic – such as for instance [NSTN93], [TNK*93] or [DNKY97] – of which we are well aware, but which we omit in this discussion. These papers also offer valuable insights into the synthesis of absolute skylight radiance values and could equally well have served as "parent" skylight models for our developments. However, since all previous papers in this area only deal with the computation of unpolarised skylight intensities we chose to only concentrate on one particular subset of them.
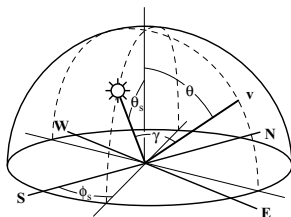
Figure 1: *Skydome coordinates and angles as used both by some of the cited skylight models and our approach. Image redrawn after [PSS99].*

Perez et al.

In the model introduced by Perez [PSM93] – which is very similar to the earlier basic skydome radiance model proposed by the CIE [CIE94] – the luminance F for a given point on the skydome is controlled by one key factor, namely the turbidity T (a numerical parameter for sky clarity):

$$\mathscr{F}(\theta,\gamma) = (1 + Ae^{B/\cos\theta})(1 + Ce^{D\gamma} + E\cos^2\gamma) \quad (1)$$

where A, B, C, D and E are distribution coefficients related to T and γ and θ are the angles shown in figure 1; we use the same convention as [PSS99]. The luminance Y for sky in any viewing direction depends on the distribution function and the zenith luminance and is given by

$$Y = Y_z \mathscr{F}(\theta,\gamma) / \mathscr{F}(0,\theta_s) \quad (2)$$

The Perez model has been found to be slightly more accurate than the widely cited basic CIE model [CIE94] if the parameters A through E are chosen wisely.

Preetham et al.

One of the most sophisticated skylight models so far is the one defined by [PSS99]. The main improvement offered by their approach is that it provides genuine spectral radiance values for each sample; in this way the varying colour hues of natural skies are taken into account. The images produced with this model are very appealing, while the required computational effort is still basically similar to the other models.

2.2. Skylight polarisation

The fact that the radiance pattern of a clear daytime sky exhibits significant amounts of linear polarisation has been known for a long time, and is still the topic of contemporary study such as [Cou88]. Several physicists of the 19th century studied the phenomenon, and – apart from qualitatively describing the shape of the polarised regions – determined the existence and location of several *neutral points*, where the emitted light is unpolarised; see figure 2 for a sketch of their location. These points are named after their discoverers: the most obvious one is the *Arago* point, which is on average $20°$ above the antisolar point and therefore only visible for low solar elevations. The *Babinet* and *Brewster* points are harder to observe, since they are both about $15°$ away from the sun in areas of very strong luminance.

It has to be noted that circular and elliptic polarisation do not normally occur on the sky, which makes the creation of analytical models much easier since only the degree of linear polarisation (as opposed to a full set of Stokes vectors, see section 2.4) has to be computed for a given viewing direction.

The amount of linear polarisation found on the sky is not constant over the entire skydome, and is strongly dependent on both the solar position and the turbidity of the atmosphere. The strongest polarisations can be observed at $90°$ from the sun during sunset on clear days; it can reach over 90% under optimal conditions, i.e. perfectly dry air with no clouds or haze whatsoever.

As a rule of thumb it can be stated that the deeper and clearer the blue of the sky is, the stronger its polarisation will be. Photographers can exploit this effect and use polarisation filters to achieve spectacularly dark blue skies in their images.

Rayleigh scattering

The mathematical foundation needed to describe the phenomenon on a molecular level is the theory of *Rayleigh*
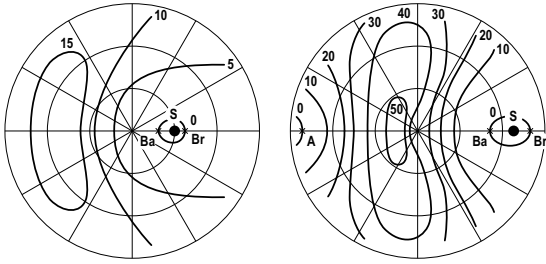
Figure 2: *Qualitative sketch of skylight polarisation levels in percent for two different solar elevations. **S** solar position, **A** Arago point, **B**r Brewster point, **B**a Babinet point. This graph was redrawn from an encyclopedia of optics [MFKS61]; the original is one of the very few such illustrations in literature, with most figures resorting to 1D line graph representations such as those found in [Lio02] or the two–dimensional but less intuitive Stokes component plots such as in [LV97]. See figure 3 for a corresponding photograph of a real sky.*

Figure 3: *Polarisation pattern of a real sky at sunset photographed through a fisheye lens with a $90°$ linear polarising filter. Note the increased contrast of the clouds in the polarised areas, and their slight influence on the shape of the polarised region.*
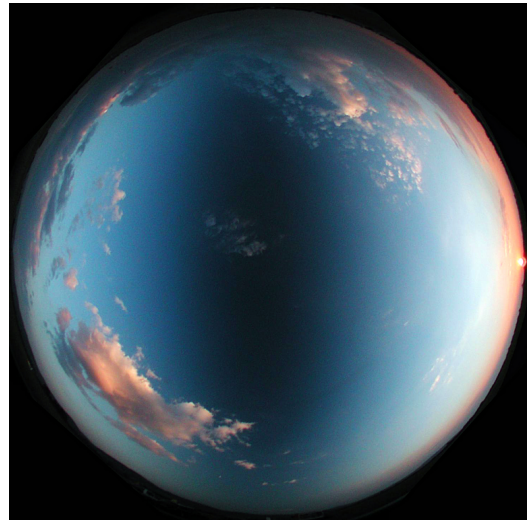
or molecular scattering. It was proposed in 1871, and was the first theory which was able to properly explain the blue colour of the sky.

A key insight was that even individual air molecules – which are significantly smaller than the wavelength of light – are capable of scattering light; previous theories had required the assumption of comparatively macroscopic particles which act as scattering agents.

This type of scattering is strongly dependent on the colour of the light in question; for a given wavelength λ the scattered intensity I_λ is roughly equivalent to $\frac{1}{\lambda^4}$. Blue light with $\lambda \approx 425$nm scatters about 5.5 times more energy away from its direction of propagation than red light with $\lambda \approx 650$nm [Lio02], which is why the sky appears blue when viewed at an angular distance from the sun.

Apart from being able to explain the colour of the sky, the theory of Rayleigh scattering also allows us to compute the degree of polarisation which is caused by the scattering process. The degree of polarisation is dependent on the scattering angle, and goes from 0.0 at $0°$ to 1.0 at $90°$ from the direction of propagation.

The reason we do not observe the total polarisation predicted by this theory for a viewing angle of $90°$ away from the sun in nature is that even the purest atmosphere generates secondary scattering events, which reduce the degree of polarisation. How far this reduction goes is dependent on the turbidity; while clear blue skies are strongly polarised, hazy skies exhibit very little polarisation.

2.3. Reflection from specular surfaces

In order to show the potentially large importance of incident light polarisation for scenes with specular surfaces, it is instructive to consider the Fresnel terms, which describe the reflected intensity for interactions of light with perfect reflectors. Since physically plausible reflection models such as [CT81] or [HTSG91] use these terms even for reflections which are not perfectly specular, the applicability of the following argument is not limited to perfect mirrors.

Fresnel Terms

In their full form (the derivation of which can e.g. be found in [SH92]), they consist of two pairs of equations, one for the reflectance, and the second for the phase retardance of the two polarisation components. Both pairs of formulas can be found in related literature, such as e.g. [WK90]; for the point we are trying to make, only the commonly used first pair for the specular reflectance is relevant.

In figure 4 we show the Fresnel reflectivity for two typical materials: one conductor, a class of materials which has a complex index of refraction and is always opaque, and one dielectric, which in pure form is usually transparent, and has a real–valued index of refraction.

The noteworthy feature of this diagram is that for certain angles of incidence around and above Brewster's angle – the angle at which reflected light is completely linearly polarised – the ratio of the reflectivities for the two polarisation types is quite large.
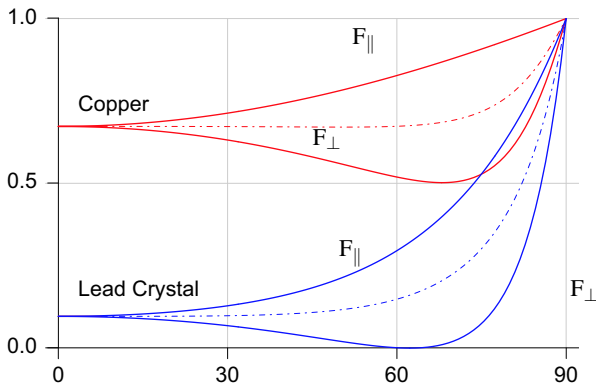
Figure 4: *Fresnel reflectivities* $F_\parallel$, $F_\perp$ *and* $F_{average}$ *(dashed lines) for copper (red) and lead crystal (blue) at 560nm. As a conductor, copper has a complex index of refraction and does not polarise incident light very strongly at Brewster's angle. For lead crystal, with its real–valued index of refraction of about 1.9, total polarisation of incident light occurs at about* $62°$. *Note the large ratio between the individual polarisation components for angles near and above Brewster's angle.*

Figure 5: *Horizontal view* $90°$ *away from the sun over a lake through a horizontal polarising filter. A fisheye lens was used for this real photo to emphasize the mirror effect caused by the skylight polarisation (which is visible as a dark band in the sky). A similar image can be found in [Kön85]. It is important to note that the dark area on the water is present even when no polarising filter is used, since reflections are not canceled out by a horizontal filter. See figure 6 for such an image.*

In conjunction with already linearly polarised incoming light this can lead to strong changes in the reflected radiance, which is why scenes with specular objects – such as water surfaces, windows or glossy painted surfaces – may exhibit large discrepancies in their reflected radiance with respect to reality when rendered beneath an unpolarised skylight model; see figure 5 for a real–world example of this phenomenon.

2.4. Rendering with Polarisation Parameters

We are aware of four publications in computer graphics literature about this topic:

- [WK90], who were the first to implement a rendering system capable of handling such effects. Their work was based on the formalisms found in [BW64], and demonstrated various effects – such as changes in highlight colour and reflected highlights – that are typical for images generated by polarisation–aware renderers.

- [TTW94], who concentrated on the rendering of anisotropic crystals with more than one optical axis and extended the techniques used by [WK90].

- [FGH99], who were the first to suggest the use of the much more easily handled Stokes vector formalism instead of the coherency matrix approach favored by the earlier authors.

- [WTP01], who also proposed using the Stokes vector for-

malism, in their case specifically because it allows one to easily incorporate fluorescence effects at the same time as polarisation information.

The main goal of these efforts was that of finding an appropriate way to describe and perform calculations with polarised light; both earlier groups of authors settled for a notation suggested by standard reference texts from physics literature, while the more recent efforts used a more practical technique from the optical community. For our work, we opted to use the Stokes vector formalism, a detailed description of which can be found either in the abovementioned papers, or in [DCWP02].

3. The Proposed Skylight Polarisation Model

3.1. Scope and Limitations

Based on the background and motivation presented in the preceding sections, we derive an analytical skylight model which serves as a useful approximation to the behaviour of real skies.

It exhibits a good correspondence with reference data such as the plots in [Lio02] or [LV97], and the only reason we cannot further demonstrate its correctness by comparing its output against atmospheric reference simulations is that no

Figure 6: *Horizontal view* $90°$ *away from the sun over a lake without a polarising filter. Similar to figure 5, a fisheye lens was used for this real photo to emphasize the mirror effect caused by the skylight polarisation. Note that the reflectivity of the clouds falls off much slower than that of the sky.*

skylight model of suitable realism and sophistication which we could have used for this purpose has been published so far.

It has also to be noted at this point that the inclusion of polarisation effects is usually not necessary to generate perfectly believable images of outdoor scenes. However, their inclusion is a significant improvement on the road towards predictive rendering of outdoor scenes, and hence improved correctness of radiometric calculations in such scenes.

And even though we cannot quantify the error incurred by comparing our model to of a (so far non–existing) reference simulation of real sky behaviour, it is safe to assert that its use certainly lowers the overall radiometric error of outdoor scene rendering, and therefore serves the purpose of demonstrating both the viability and necessity of the concept of outdoor scene polarisation rendering well.

3.2. Model Components

For such an analytical model three key items are needed; we will discuss each of these in detail in the following sections.

1. An expression which describes the relative degree of polarisation at any given point in the sky depending on the position of the sun; we refer to this as the *polarisation pattern*.

2. An expression which yields the *maximum degree of polarisation* in the sky; this determines the impact of the

pattern on the skydome. This value is dependent on both the solar elevation and the turbidity.

3. A way to determine the reference coordinate system for the polarised radiation of each skylight ray, and a resulting expression for the Stokes vector based on items 1 and 2.

3.3. The Polarisation Pattern

An exact brute force simulation of the scattering processes involved in skylight luminance was not really an option for performance reasons, so we decided to devise a heuristic technique which is based on two components.

The key observations are that skylight polarisation is mainly dependent on

- the angle between the viewing direction and the sun, and the resulting linear polarisation due to Rayleigh scattering, and

- the "clearness" of the sky in the viewing direction, which influences the amount of polarisation emanating from a given direction.

We assemble the proposed model as a combination of two components which cover these properties in turn.

Polarisation due to scattering

To determine the relative degree of polarisation the term for linear polarisation due to Rayleigh scattering given in [Lio02] is used for the first of the components.

$$LP(\theta) = \frac{1 - \cos^2\theta}{1 + \cos^2\theta} = \frac{\sin^2\theta}{1 + \cos^2\theta} \qquad (3)$$

where θ is the scattering angle (i.e. the angle by which a ray of light is diverted when interacting with a particle).

The influence of skylight intensity

In order to obtain the degree of polarisation, the inverse of the skylight intensity is taken as a basis. This is justifiable since there is an indirect connection between the degree of polarisation and skylight intensity: for low sun positions the deep blue regions near the zenith are strongly polarised, whereas the brighter regions near the horizon exhibit significantly weaker polarisation. A suitable expression for this behaviour is

$$I(\gamma, \theta) = \left(\frac{1}{I_{perez}} - \frac{1}{I_{sun}} \right) \frac{I_{90}\ I_{sun}}{I_{sun} - I_{90}} \qquad (4)$$

where I_{perez} is the intensity according to the Perez model and I_{90}, I_{sun} are the intensity values at $90°$ from the sun and for looking directly at the sun; in this way the intensity is inverted and normalized.

The influence of sky clarity

The base degree of polarisation given in equation 4 needs to be modified to incorporate the lessening of polarisation effects due to aerosols near the horizon. Therefore we need a function which has its maximum at the zenith and decreases towards the horizon; we found a simple cosine dependency to be sufficient for this purpose:

$$E(\theta) = \cos(\theta) \qquad (5)$$

The combined pattern model

These two components are combined in such a way that equation 4 is preferred at the zenith and equation 5 is preferred at the horizon. This results in the following expression for the polarisation pattern:

$$P(\gamma, \theta) = \frac{1}{C} LP(\gamma) \left(\theta \cos(\theta) + \left(\frac{\pi}{2} - \theta \right) I(\gamma, \theta) \right) \qquad (6)$$

where C is an empirical scaling constant of 1.2 which ensures that the maximal values of this expression – which occur for solar elevations of $0°$ – are not larger than 1.0.

Sample plots of the pattern generated by this formula can be seen in figure 7; the similarity to the patterns seen in figures 2 and 3 is evident.
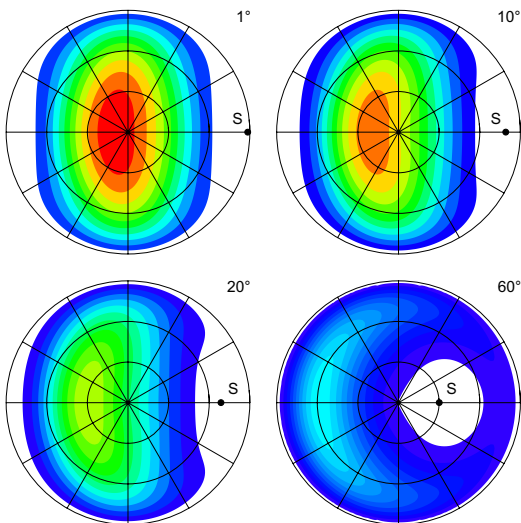

Figure 7: *Plots of the patterns generated by the proposed model for a low turbidity and solar elevations of 1, 10, 20 and 60 degrees, respectively. Red areas exhibit the highest levels of linear polarisation, while white areas are unpolarised. The changes in maximal polarisation for varying solar angles shown in these plots corresponds to the differences shown in figure 8. Compare them to the patterns shown in figure 2.*

The relative degree of polarisation which this pattern formula provides for different solar elevations can be seen from

figure 8; in order to faciliate proper scaling by the factor determined in section 3.4, the scaling by C is done to reach a maximum value of 1.0 for all turbidities.

Our proposed model for skylight polarisation approximates actual measurements [Lio02] very well: the cross sections shown in figure 8 agree with the cited observations at the Mauna Loa Obsevatory.
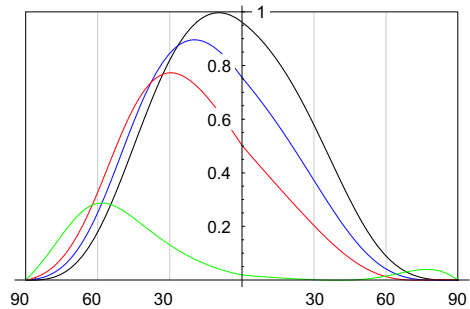
Figure 8: *Plots of the relative degree of polarisation for the four diagrams in figure 7. The green curve is a cut through the symmetry axis of the pattern at $60°$, red for $20°$, blue for $10°$ and black for $1°$ solar elevation. This diagram is similar to the figures used e.g. in [Lio02], and shows that our pattern formula P already includes the influence of solar elevation on the degree of polarisation.*

3.4. Maximum degree of polarisation

Our approach uses a hybrid formula for the polarisation pattern, since P already includes the influence of solar elevation; because of this we only have to consider the influence of the turbidity on the overall degree of polarisation here.

The type of relationship between turbidity and the maximal degree of polarisation is comparatively obvious (an exponential falloff for rising turbidity values similar to the maximal viewing distance), but hard to quantify in an exact fashion due to the intricacies of the interactions between light and the many layers found in real atmospheric conditions.

Papers on the subject such as [Cou83] usually just present measurements for particular dates, locations and environmental settings. Due to the complexity of the subject these papers normally do not provide an analytical description of the phenomena they measured.

We therefore propose to use a simple empirically determined formula for the maximal degree of polarisation M_p which provides a suitable gradual exponential falloff for rising values of the turbidity T.

$$M_p(T) = e^{-\frac{T - C_1}{C_2}} \qquad (7)$$

The constants C_1 and C_2 are used to fit the curve – an example of which is shown in figure 9 – to a plausible shape

that agrees with individual values mentioned in literature. A useful pair of values for C_1 and C_2 is e.g. $(0.6, 4.0)$.
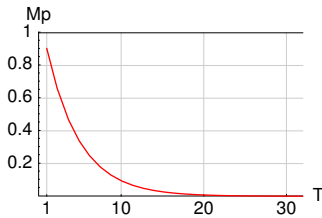
Figure 9: *Plot of the exponential falloff of the maximum degree of polarisation for turbidities in the range from 1 to 32 and values of $(0.6, 4.0)$ for $C_{1,2}$. The almost complete disappearance of M_p for high turbidity values corresponds to the fact that no polarisation is apparent on very hazy days.*

This approximation is permissible insofar as a) the polarisation patterns generated by the proposed model are a good approximation (as opposed to an exact solution) to begin with, b) the exponential falloff behaviour exhibited by the formula is qualitatively correct and also c) because this property of the model can easily be controlled by the user through the factors C_1 and C_2 if a different behaviour is desired.

3.5. Putting it together: the skylight Stokes vector

Apart from actually assembling the Stokes vector for a given skylight sample, we also have to determine the *reference system* for the polarisation information we have computed. In a polarisation–aware renderer, all rays have to maintain their own reference coordinate system, since the Stokes parameters are only meaningful for a given geometrical context.

A suitable reference system can be constructed as follows: the vector product of the view direction v and the solar position vector (see figure 1) yields a vector which is normal to the propagation of light from the sun through the atmosphere. This vector is the first basis of the reference system, and the second can be obtained through a vector multiplication of this vector with the viewing direction. If needed, the third can be obtained from these two vectors, again through a vector product.

If this reference system is used, assembly of the actual Stokes vector is straightforward. The proposed model yields the degree of linear polarisation D (equation 9) – which corresponds to the second Stokes parameter in our reference system – for a given viewing direction as a value in the interval $[0,1]$. If the unpolarised spectral radiance for this direction is R, this information can be directly translated to a

set of Stokes parameters:

$$\begin{aligned} E_0 &= R \\ E_1 &= D \cdot R \\ E_2 &= 0 \\ E_3 &= 0 \end{aligned} \qquad (8)$$

The value for R is provided by the "parent" skylight model, such as the technique of [PSS99], and D is determined through the combination of P and M_p

$$D(\gamma, \theta, \sigma, T) = M_p(T) \cdot P(\gamma, \theta, \sigma, T) \qquad (9)$$

3.6. Aerial perspective

So far we have only discussed the polarisation of directly observed skylight radiances, but any realistic skylight model has to include a computation of haze and inscattered radiance into the view ray. For instance, the approach presented by [PSS99] is a good tradeoff between accuracy and computability within a reasonable timeframe, and provides formulas for the attenuation through haze and scattering as well as expressions for the inscattering of light into a ray path.

While the attenuation component is more or less unpolarised, the inscattered light can exhibit a certain amount of polarisation; this effect is sometimes used by landscape photographers to improve the clarity of distant features. Since the processes which lead to inscattering are similar for both directly observed skylight and the inscattering component which is used for haze computations, we opted to use the same expression for the degree of polarisation of this quantity as for the directly observed skydome radiances. This provides a useable approximation at a fraction of the cost which a real scattering simulation would require.

Even for very clear skies our model yields rather low degrees of polarisation for horizontal directions which are typically associated with aerial perspective; however, this is consistent with reality insofar as the polarisation of aerial perspective effects is never particularly strong even under favorable conditions.

3.7. Applicability

In principle the proposed model can trivially be used to provide any of the skylight models discussed in section 2.1 (and probably most others as well) with a polarisation component; it is not dependent on the "parent" model in any way. Due to this it can also be employed to provide Stokes vector information to empirical techniques such as high dynamic range image skylights, e.g. those used by [Deb98], or other analytical high–quality skylight models such as those which were derived by [NSTN93] or [TNK*93].

4. Results

We implemented the proposed model in the context of a polarisation–aware spectral path tracer. The "parent" skylight model used was the one proposed by [PSS99]. Since the implementation of this model predated this research effort, we only had to add the polarisation expressions described in section 3.5 to the existing code, and perform our experiments.

4.1. Test cases

The test renderings in figure 10 show fisheye views of the entire sky for different turbidities. Figure 11 visualizes the degree and orientation of the linear polarisation in these figures; figure 13 explains the false colour scheme which is used here and in figure 14 (e).
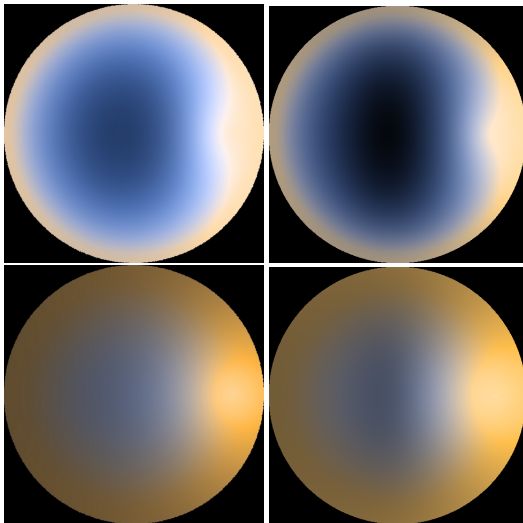

Figure 10: *Fisheye views of the entire skydome using Preetham's model augmented with our polarisation model for a solar elevation of $15°$ and a turbidity of 2 (top) and 6 (bottom). The left image is the plain view, while the right one had a linear polariser applied to it to yield a visualization of the polarised region. Compare this to figure 3; the much lower degree of polarisation in the case of turbidity 6 is due to the correction factor from equation (7).*

The test scene used in figure 14 was chosen as a typical example of an outdoor scene with a large number of specular interreflections. We demonstrate that noticeable differences in the appearance of such objects occur when polarisation is taken into account by rendering the scene in three configurations and examining the differences between the results.

In the first configuration we used a standard (nonpolarising) renderer (a), and for the second test we used both a polarisation renderer and our proposed model (b).

In order to properly estimate the difference which a polarised skylight makes within the context of a polarising renderer we also performed a third test and rendered the scene using a polarising system, but with a normal, unpolarised skylight model (c)
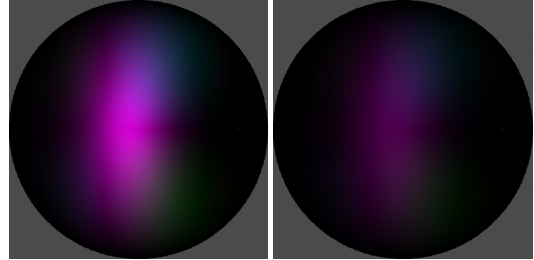
Figure 11: *False colour renderings of the orientation and degree of polarisation in the skydomes seen in figures 10; left is turbidity 2, right turbidity 6. The brighter the pink colour, the higher the degree of polarisation. The colour (and hence orientation) variations are due to the nonlinear projection of the skydome performed by the fisheye camera.*

A difference image between the result of the plain rendering and the fully polarising case is shown in figure 14 (d). Also, figure 14 (e) uses the same false–colour scheme as figure 10 to visualize the amount and orientation of the linear polarisation which is present in the result generated by test configuration 2. The most strongly polarised parts of the image are the reflections in the water and at the top of the skyscrapers.

The second difference image – shown in figure 14 (f) – was computed between the results of the configuration 1: polarised skylight/polarisation renderer, and configuration 3: unpolarised skylight/polarisation renderer. It demonstrates that while configuration 3 is naturally able to compute the interreflections between the skyscrapers and the water to a higher standard than configuration 1, the omission of the polarisation information on the skydome leads to considerable differences compared to the full simulation.

It has to be noted that the differences between the various result images are a bit hard to judge visually due to the loss of information through the necessary tone reproduction step; only the difference images provide reliable information in this respect.

4.2. Performance

The renderer we used is a hybrid system that optionally can be compiled to include polarisation support. This enabled us to perform meaningful side–by–side comparisons of both types of renderer since essentially the same codebase is used in both cases. For the presented test scene the used spectral rendering system performed as follows: the fully polarised solution (i.e. case 2) took about twice as long to compute as the plain nonpolarised case (10 vs. 20 minutes on an Athlon

2400+). This not particularly excessive increase in computation time is due to the fact that starting with moderately complex environments such as the skyscraper scene (it consists of approximately 7k CSG primitives) ray intersection calculations – and not the quite costly polarisation–aware reflectancy and light manipulations – already make up the majority of the expended computational effort.

a)   b)

c)
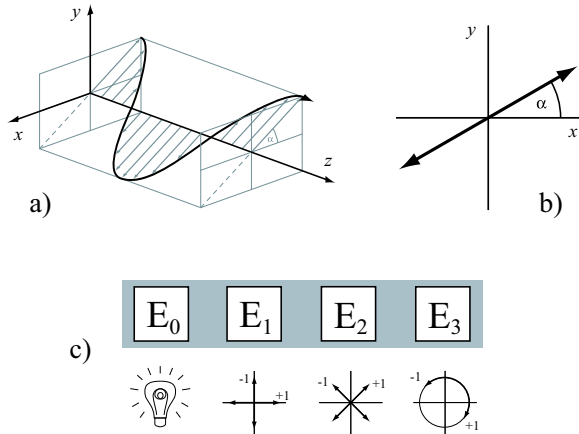
Figure 12: *a) Three-dimensional view of the propagation of a linearly polarised lightwave which is rotated by an angle of* α *from the x-axis. b) Two-dimensional view of the plane of oscillation for this wave. c) The Stokes Vector formalism: four numbers are used to describe the polarisation state of a wave. The first component* E_0 *encodes the total luminance, components* E_1 *and* E_2 *encode linear polarzation in two different orientations rotated by* $45°$*, and* E_3 *is used to describe the circular polarisation component.*

a)   b)
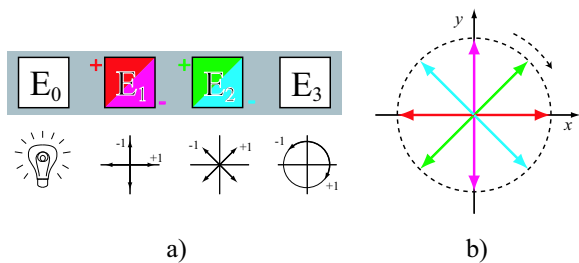
Figure 13: *Explanation of the false colour scheme used in this paper to display linear polarisation. a) Assignment of colours to components 1 and 2 of the Stokes vector. Red and green are used to encode the percentage of polarisation for each of these components, with blue being added if the component is negative. b) The resulting colours for several planes of oscillation. Note that this scheme intentionally omits circular polarisation (dashed circle), since it usually does not appear in scenes which are illuminated by skylight, and also omits all absolute radiance information.*

The hybrid case 3 with an unpolarised skylight model was

noticeably – although not dramatically – faster than case 2 (it was only 1.7 times slower than case 1). This can be explained by the fact that the system performs optimizations which switch to the cheaper calculations for unpolarised light if the possibility presents itself, which it does more often in this case.

However, this still shows that the large increase in realism offered by the polarised skylight model comes at such a comparatively small cost that its omission would not make sense within a polarisation–aware renderer, especially since one would not use such a system for renderings where accuracy does not have a high priority.

5. Conclusion and Future Work

We have defined a simple analytical approach to providing qualitatively correct polarisation patterns to existing skylight models, and demonstrated its utility on a suitable outdoor test scene. It is intentionally described in a very algorithmic way, which should make it easy for programmers to implement it within any appropriate renderer.

While the output of the proposed model is not entirely physically correct in the strict sense – it is e.g. not capable of representing the neutral points of skylight polarisation – it is nonetheless sufficient for most rendering applications, since its features cover all the *noticeable* aspects of skylight polarisation to a sufficient degree.

Subtleties like the neutral points can be hard to detect even with appropriate instrumentation, and their absence does not alter the appearance of outdoor scenes in a perceivable way.

Our future efforts will nonetheless go into the direction of attempting to find more accurate descriptions of the polarisation pattern, and to obtain a more physically plausible expression for M_p. Also, we will attempt to derive a more finely controllable overall skylight model which will feature the polarisation information as an integral part of the computed spectral luminance information and which is consequently capable of exhibiting wavelength–dependent polarisation effects.

Acknowledgements

References

[BW64]   BORN M., WOLF E.: *Principles of Optics*. The Macmillan Company, 1964.

[CIE94]   CIE-110: Spatial distribution of daylight - luminance distributions of various reference skies. *Tech. rep., International Commission of Illumination* (1994).

[Cou83]   COULSON K. L.:   Effects of the el chichon volcanic cloud in the stratosphere on the polarization of light from the sky. *Applied Optics* (1983).

[Cou88]   COULSON K. L.: *Polarization and Intensity of Light in the Atmosphere*. A. Deepak Publishing, 1988.

[CT81]   COOK R. L., TORRANCE K. E.: A reflectance model for computer graphics. *Computer graphics, Aug 1981 15*, 3 (1981), 307–316.

[DCWP02] DEVLIN K., CHALMERS A., WILKIE A., PURGATHOFER W.:   STAR: Tone reproduction and physically based spectral rendering. In *State of the Art Reports, Eurographics 2002* (Sept. 2002), Fellner D., Scopignio R., (Eds.), The Eurographics Association, pp. 101–123.

[Deb98]   DEBEVEC P.:   Rendering synthetic objects into real scenes: Bridging traditional and image-based graphics with global illumination and high dynamic range photography.   In *SIGGRAPH 98 Conference Proceedings* (July 1998), Cohen M., (Ed.), Annual Conference Series, ACM SIGGRAPH, Addison Wesley, pp. 189–198. ISBN 0-89791-999-8.

[DNKY97] DOBASHI Y., NISHITA T., KANEDA K., YA-MASHITA H.:   A fast display method of sky colour using basis functions. In *The Journal of Visualization and Computer Animation* (1997), Thalmann N. M., Thalmann D., Shin S. Y., Kunii T. L.,, Kim M.-S., (Eds.), vol. 8(2), John Wiley & Sons, Ltd., pp. 115–127.

[FGH99]   FRENIERE E. R., GREGORY G. G., HASSLER R. A.: Polarization models for monte carlo ray-tracing. *Proceedings of SPIE 3780* (1999).

[HG83]   HALL R. A., GREENBERG D. P.:   A testbed for realistic image synthesis. *IEEE Computer Graphics and Applications 3*, 8 (Nov. 1983), 10–20.

[HTSG91] HE X. D., TORRANCE K. E., SILLION F. X., GREENBERG D. P.: A comprehensive physical model for light reflection. *Computer Graphics 25*, 4 (July 1991), 175–186.

[Kön85]   KÖNNEN G. P.: *Polarized Light in Nature*. Cambridge University Press, 1985.

[Lio02]   LIOU K. N.: *An Introduction to Atmospheric Radiation*. Academic Press, 2002.

[LV97]   LIU Y., VOSS K.:   Polarized radiance distribution measurement of skylight. ii. experiment and data. *Applied Optics* (1997).

[MFKS61] MÜTZE   K.,   FOITZIK   L.,   KRUG   W.,   SCHREIBER   G.:   *ABC der Optik*.   VEB Edition, Leipzig, DDR, 1961.

[NSTN93] NISHITA T., SIRAI T., TADAMURA K., NAKAMAE E.: Display of the earth taking into account atmospheric scattering. In *Computer Graphics (SIGGRAPH '93 Proceedings)* (Aug. 1993), Kajiya J. T., (Ed.), vol. 27, pp. 175–182.

[PFFG98] PATTANAIK S. N., FERWERDA J. A., FAIRCHILD M. D., GREENBERG D. P.:   A multiscale model of adaptation and spatial vision for realistic image display. In *SIGGRAPH 98 Conference Proceedings* (July 1998), Cohen M., (Ed.), Annual Conference Series, ACM SIGGRAPH, Addison Wesley, pp. 287–298. ISBN 0-89791-999-8.

[PSM93]   PEREZ R., SEALS R., MICHALSKY J.:   All-weather model for sky luminance distribution - preliminary configuration and validation. *Solar Energy 50*, 3 (1993), 235–245.

[PSS99]   PREETHAM A. J., SHIRLEY P., SMITS. B. E.: A practical analytic model for daylight. In *Siggraph 1999, Computer Graphics Proceedings* (Los Angeles, 1999), Rockwood A., (Ed.), Annual Conference Series, ACM Siggraph, Addison Wesley Longman, pp. 91–100.

[SH92]   SIEGEL R., HOWELL J. R.: *Thermal Radiation Heat Transfer, 3rd Edition*.   Hemisphere Publishing Corporation, New York, NY, 1992.

[TNK*93] TADAMURA K., NAKAMAE E., KANEDA K., BABA M., YAMASHITA H., NISHITA T.: Modeling of skylight and rendering of outdoor scenes.   *Computer Graphics Forum 12*, 3 (1993), C189–C200.

[TTW94]   TANNENBAUM D. C., TANNENBAUM P., WOZNY M. J.: Polarization and birefringency considerations in rendering. In *Proceedings of SIGGRAPH '94 (Orlando, Florida, July 24–29, 1994)* (July 1994), Glassner A., (Ed.), Computer Graphics Proceedings, Annual Conference Series, ACM SIGGRAPH, ACM Press, pp. 221–222. ISBN 0-89791-667-0.

[WK90]   WOLFF L. B., KURLANDER D.:   Ray tracing with polarization parameters. *IEEE Computer Graphics & Applications 10*, 6 (Nov. 1990), 44–55.

[WTP01]   WILKIE A., TOBLER R. F., PURGATHOFER W.:   Combined rendering of polarization and fluorescence effects. In *Proceedings of the 12th Eurographics Workshop on Rendering* (London, UK, June 25–27 2001), Gortler S. J., Myszkowski K., (Eds.), pp. 197–204.
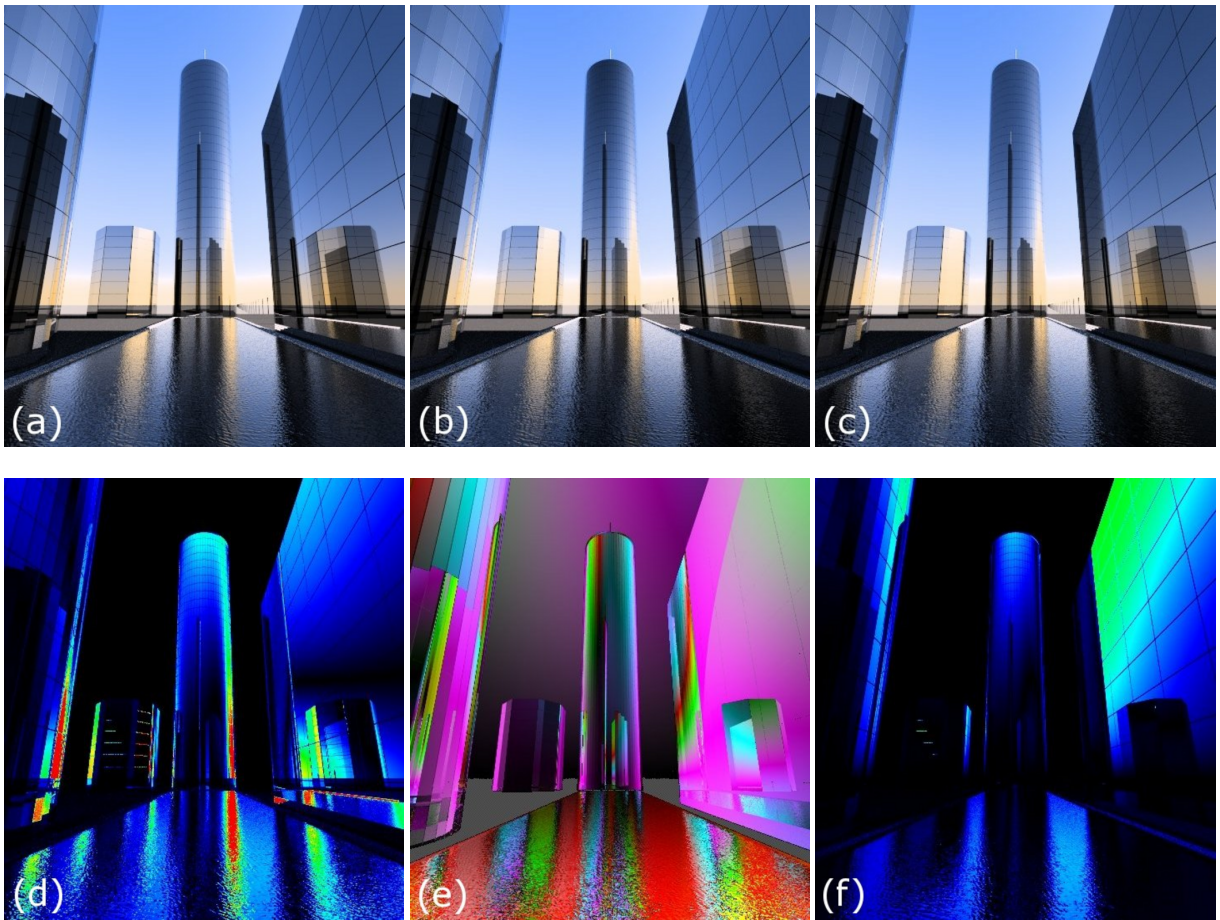
Figure 14: *A sample outdoor scene with a large number of highly specular surfaces.* (a) *This image was rendered with a plain rendering engine.* (b) *The same scene, but rendered using a polarisation-aware engine. A number of differences – e.g. near the top of the central skyscraper or in the reflection on the water – are apparent; figure (d) shows a difference image which helps to locate areas of interest.* (c) *same scene as in (b), but this time rendered using a polarisation-aware engine* without *a polarised skylight.* (d) *Difference image of the two renderings in (a) and (b). The main differences are to be found in the reflection of the central skyscraper in the water and at the top of the main skyscraper.* (e) *False colour rendering of the polarisation for each pixel in (b); the false colour scheme is explained in Figure 13. Note that most specular surfaces exhibit a very strong polarisation.* (f) *Difference image of the two renderings in figures (b) and (c).*